doi:10.1093/brain/awab141 BRAIN 2021: 144; 2863–2878 | 2863

BRAIN
ORIGINAL ARTICLE

Kcnq2/K_v7.2 controls the threshold and bi-hemispheric symmetry of cortical spreading depolarization

Isamu Aiba and Jeffrey L. Noebels

Spreading depolarization is a slowly propagating wave of massive cellular depolarization associated with acute brain injury and migraine aura. Genetic studies link depolarizing molecular defects in Ca^{2+} flux, Na^+ current in interneurons, and glial Na^+-K^+ ATPase with spreading depolarization susceptibility, emphasizing the important roles of synaptic activity and extracellular ionic homeostasis in determining spreading depolarization threshold. In contrast, although gene mutations in voltage-gated potassium ion channels that shape intrinsic membrane excitability are frequently associated with epilepsy susceptibility, it is not known whether epileptogenic mutations that regulate membrane repolarization also modify spreading depolarization threshold and propagation.

Here we report that the Kcnq2/K_v7.2 potassium channel subunit, frequently mutated in developmental epilepsy, is a spreading depolarization modulatory gene with significant control over the seizure-spreading depolarization transition threshold, bi-hemispheric cortical expression, and diurnal temporal susceptibility. Chronic DC-band cortical EEG recording from behaving conditional *Kcnq2* deletion mice ($Emx1^{cre/+}$::$Kcnq2^{flox/flox}$) revealed spontaneous cortical seizures and spreading depolarization. In contrast to the related potassium channel deficient model, K_v1.1-KO mice, spontaneous cortical spreading depolarizations in *Kcnq2* cKO mice are tightly coupled to the terminal phase of seizures, arise bilaterally, and are observed predominantly during the dark phase. Administration of the non-selective K_v7.2 inhibitor XE991 to K_v1.1-KO mice partly reproduced the *Kcnq2* cKO-like spreading depolarization phenotype (tight seizure coupling and bilateral symmetry) in these mice, indicating that K_v7.2 currents can directly and actively modulate spreading depolarization properties. *In vitro* brain slice studies confirmed that Kcnq2/K_v7.2 depletion or pharmacological inhibition intrinsically lowers the cortical spreading depolarization threshold, whereas pharmacological K_v7.2 activators elevate the threshold to multiple depolarizing and hypometabolic spreading depolarization triggers.

Together these results identify Kcnq2/K_v7.2 as a distinctive spreading depolarization regulatory gene, and point to spreading depolarization as a potentially significant pathophysiological component of KCNQ2-linked epileptic encephalopathy syndromes. Our results also implicate KCNQ2/K_v7.2 channel activation as a potential adjunctive therapeutic target to inhibit spreading depolarization incidence.

Department of Neurology, Baylor College of Medicine, Houston, TX 77030, USA

Correspondence to: Isamu Aiba
Department of Neurology, Baylor College of Medicine
One Balyor Plaza, Houston, TX 77030, USA
E-mail: aiba@bcm.edu

Correspondence may also be addressed to: Jeffrey L. Noebels
E-mail: jnoebels@bcm.edu

Received November 27, 2020. Revised February 22, 2021. Accepted March 20, 2021. Advance access publication March 26, 2021
© The Author(s) (2021). Published by Oxford University Press on behalf of the Guarantors of Brain.
This is an Open Access article distributed under the terms of the Creative Commons Attribution-NonCommercial License (http://creativecommons.org/licenses/by-nc/4.0/), which permits non-commercial re-use, distribution, and reproduction in any medium, provided the original work is properly cited. For commercial re-use, please contact journals.permissions@oup.com

Keywords: epilepsy; seizure; K_v1.1; retigabine; XE991

Abbreviations: IOS = intrinsic optical signal; OGD = oxygen-glucose deprivation; sEPSC = spontaneous excitatory postsynaptic current; sIPSC = inhibitory postsynaptic current

Introduction

Spreading depolarization is a slow-moving wave of cellular depolarization in the brain grey matter associated with human neurological deficits in the setting of acute traumatic brain injury, ischaemic/haemorrhage stroke, migraine with aura, and other conditions.[1–6] Recent experimental studies also implicate spreading depolarization in sudden unexpected death in epilepsy (SUDEP[7–9]) and early epileptogenesis in glioblastoma.[10] While the exact inciting mechanisms remain to be elucidated and could vary across different clinical settings, spreading depolarization begins as a localized severe depolarization of brain tissue that profoundly elevates the extracellular concentration of excitatory solutes such as potassium and glutamate, which defuse and further depolarize surrounding tissue, creating a self-regenerative, spreading wave of cellular depolarization and oedema.[1] Cellular depolarization during spreading depolarization is so severe that transmembrane ionic gradients fail, transiently silencing the activity of affected networks or causing permanent damage when brain tissue is metabolically compromised.[11,12] Spreading depolarization may remain clinically silent, or promote malignant neurovascular inflammation that may contribute to longer lasting neurological deficits.[13,14]

Seizures and spreading depolarization are related excitatory events and can be generated alone or in temporally associated manners in isolated brain slices, intact and injured brains, and computational simulations.[15–20] Cortical seizures elevate extracellular K^+ concentration to a ceiling level of 7–14 mM,[21–23] a concentration range close to the spreading depolarization threshold,[1,24] sometimes leading to secondary generation of spreading depolarization.[8,16,25] Spreading depolarization arising secondary to a seizure may contribute to postictal complications such as migraine and hemiplegia (e.g. Todd's paralysis[26]) whereas spreading depolarization preceding a seizure may underlie migraine-related seizures. However, not all seizures are associated with spreading depolarization, and epilepsy patients do not always display perictal spreading depolarization-related deficits. While their relationship is complex, no molecular determinants for this seizure-spreading depolarization coupling threshold have yet been identified.

The growing identification of genes causally assigned to clinically defined epilepsy syndromes is providing decisive mechanistic insight into the molecularly diverse pathogenesis of seizure disorders. Similarly, while fewer in number, genetic analysis of complicated migraine with aura syndromes such as familial hemiplegic migraine (FHM) revealed molecular mechanisms underlying spreading depolarization threshold and susceptibility. The genes identified in FHM to date share a risk of developmental epileptic comorbidity via distinct mechanisms, including calcium current facilitation of synaptic glutamate release (FHM1: *CACNA1A*[27,28]) impaired extracellular K^+ and glutamate clearance (FHM2: *ATP1A2*[29–32]) and defective inhibitory neuron excitability (FHM3: *SCN1A*[33–35]). These genes assign a spreading depolarization threshold-determining role to excitatory/inhibitory synaptic function and ionic homeostasis in the interstitial space. In epilepsy, mutations in genes regulating intrinsic membrane excitability, including *SCN1A*, are a common cause of epilepsy with a wide range of phenotypic severity. Given the distant relationship between seizure and spreading depolarization, genes among this group may also contribute to spreading depolarization threshold, however it is not known whether they generate distinctive spreading depolarization phenotypes.

Toexplore the influence of intrinsic membrane excitability defects, we evaluated the ability of the Kcnq2/K_v7.2 channel activity to affect cortical spreading depolarization using a viable conditional *Kcnq2* knockout (KO) mouse model (Kcnq2-cKO:Emx1-cre::Kcnq2$^{flox/flox}$) and synthetic Kcnq2 channel modulators. *Kcnq2* encodes the potassium channel subunit K_v7.2 that forms heterotetramers in axon membranes and generates non-inactivating hyperpolarizing M-type K^+ current to set the resting membrane potential.[36,37] Mutations in human *KCNQ2* are associated with a phenotypic spectrum of neonatal-onset epilepsies extending from benign neonatal to severe developmental encephalopathy[38,39–41] We combined *in vivo/vitro* electrophysiology and Kcnq2 pharmacology to examine spreading depolarization characteristics of Kcnq2-cKO mice and compare them with a second axonal potassium channel seizure model, K_v1.1 deficient mice. Our recordings from K_v1.1-KO and Kcnq2-cKO mice identified significant differences in their cortical spreading depolarization phenotypes as well as a direct interdependence of these two axonal potassium channels on spreading depolarization threshold.

Materials and methods

Animals

All animal experimental protocols were approved by Baylor College of Medicine IACUC. Experiments were conducted on wild-type C57BL6J, Emx1-cre::Kcnq2flox/flox conditional KO (Kcnq2-cKO) mouse lines. Kcnq2-flox mice were a gift of Dr A. Tzingounis.[42] Emx1-IRES-cre (JAX Stock No: 005628) mice were purchased from the Jackson Laboratory. K_v1.1 KO mice (Tac:N:NIHS-BC) were obtained from the BCM breeding colony [also available from Jackson laboratory (JAX Stock No: 003532)]. All animals were housed and bred in the Center of Comparative Medicine at Baylor College of Medicine.

Study design and statistics

In vivo DC monitoring sessions were carried out to capture at least 20 spontaneous spreading depolarization events. In total, 16 Kcnq2 and eight K_v1.1-KO and -WT (wild-type) mouse pairs were implanted, while four Kcnq2-cKO mice were excluded because of poor post-surgical recovery or damage at the implant site. The identity of the mouse genotype was not blinded as it could be behaviourally identified during careful monitoring; however, the EEG data were reviewed by two experienced investigators.

In vitro acute brain slice experiments were carried out in a blinded manner by masking the identity of the tissue genotype, and due to this experimental design, *n* is not always equal between groups. In order to reduce the number of animals and increase statistical power, most *in vitro* drug experiments involved repeated measurements. Because of the robust pharmacological and genetic effects, we set a minimum $n = 6$ for independent comparisons and

$n = 4$ for repeated measurements in the same slice. *In vivo* anaesthetized mouse experiments were repeatedly performed in each mouse to increase the statistical power. In these studies, latency differences between the onset of the first (baseline) and second (drug) evoked spreading depolarization were compared.

All statistical comparisons were made using an unpaired *t*-test for two-group comparisons and repeated measures ANOVA with *post hoc* Tukey's multiple comparisons test unless mentioned. Statistics were computed using Graphpad Prism (GraphPad) and R software. All data are presented as mean ± standard deviation (SD). Imaging data were analysed using ImageJ software.

Acute brain slice preparation

Mice were deeply anaesthetized with intraperitoneal avertin (bromoethanol) followed by intracardiac perfusion with 10 ml of dissection solution (110 mM NMDG, 8 mM $MgSO_4$, 25 mM $NaHCO_3$, 1.25 mM Na_2HPO_4, 3 mM KCl, 10 mM glucose, 0.4 mM ascorbate, saturated with 95% O_2/5% CO_2 gas), and then decapitated. The brain was extracted into ice-cold dissection solution, sagitally hemisected, and 300 μm coronal slices were cut on a vibratome (Leica 1300 s) and the ventral portion was trimmed. Slices were incubated in dissection solution for 5 min at 33°C, then transferred to a submerged slice chamber and maintained in artificial CSF (in mM: 130 mM NaCl, 3 mM KCl, 25 mM $NaHCO_3$, 1.25 mM Na_2HPO_4, 10 mM glucose, 0.4 mM ascorbate, saturated with 95% O_2/5% CO_2 gas) at room temperature. All *in vitro* recordings were made at 32–33°C.

Recurrent spreading depolarization generation was difficult to reproducibly trigger in a wild-type cortical slice bathed in normal artificial CSF. Therefore, to facilitate spreading depolarization generation with recoverability, we elevated the potassium chloride (KCl) concentration of artificial CSF from 3 mM to 5 mM throughout the experiments.

Models of spreading depolarization generation and detection in *in vitro* acute brain slices

In separate experiments, cortical spreading depolarization was induced by KCl bath application, KCl microinjection, Mg^{2+} free bath solution, and exposure to oxygen-glucose deprivation (OGD) solution. In all three models, spreading depolarizations were generated and detected using a glass electrode (1–2 MΩ, filled with artificial CSF) placed in cortical layer 2–3 (50 μm depth) while simultaneously monitoring the intrinsic optical signal changes (IOS, i.e. light transparency increase due to tissue swelling) using a CCD camera (DMK27BU, Imaging Source, acquisition rate: 0.2–0.5 Hz). Spreading depolarization onset was determined by detecting the IOS signal coincident with the electrophysiological depolarization within the imaging field. Spreading depolarization propagation rate was calculated by tracking the propagating wavefront over time. Imaged data of spreading depolarization propagation were converted to the ratio ($\Delta I/I_0$). Since a DC shift was not always detected if the spreading depolarization faded before reaching the recording electrode, most spreading depolarization latency and propagation parameters were based on IOS signals.

Bath KCl application was conducted by incrementally increasing the bath KCl concentration. Pairs of cortical slices were incubated in a chamber and monitored as they were serially exposed to artificial CSF containing elevated KCl (10 to 14 mM, 1 mM increment, 5 min each). The KCl concentration that triggered spreading depolarization was considered as the threshold.

In some experiments, KCl microinjection was used to trigger spreading depolarization to characterize its propagation pattern in the physiological KCl concentration. A single injection of 1 M KCl was pressure ejected via a micropipette placed in layer 2/3 using a picospritzer (pressure: 40 psi, pulse duration: 100–500 ms, estimated ejection volume: ~20 nl). In other slices, spreading depolarization was triggered by exposure to nominally Mg^{2+}-free artificial CSF in which $MgSO_4$ was eliminated in the artificial CSF without compensation of the bath divalent cation concentration.

Finally, some slices were challenged metabolically using OGD. OGD spreading depolarizations were induced by superfusing the cortical slices in the artificial CSF equilibrated with 95%N_2/5%CO_2 and reduced glucose concentration (0–5mM glucose concentration osmotically balanced to 10 mM with sucrose). For pharmacological tests, slices were pre-incubated for 5–10 min in artificial CSF containing the test compound, and then further exposed to OGD solution containing the same test compound.

In vitro electrophysiology

Spontaneous excitatory and inhibitory postsynaptic currents (sEPSC and sIPSC) were analysed using the standard patch-clamp technique as described previously.[8] Briefly, the somatosensory layer 2–3 cortical pyramidal neurons were whole-cell recorded with micropipettes (2–4 MΩ) containing a Cs-gluconate-based solution. Spontaneous postsynaptic currents in each neuron were recorded at –70 mV and 0 mV, respectively, and analysed using pClamp software (Molecular devices).

In vivo cortical spreading depolarization activity in anaesthetized mice

For acute (non-survival) *in vivo* studies, mice were anaesthetized by intraperitoneal injection of urethane (1.5 mg/kg). A craniotomy (1.0 mm diameter) was made over the somatosensory cortex and covered with a Gelfoam® pledget soaked with saline. A thinned skull region was created 2 mm anterior to the cranial window and ~0.1 mm silver wire was placed for electrophysiological DC recording. To reduce the variability of tissue oxygenation, a flow of O_2 was supplied to the nares. All mice showed an oxygen saturation (SpO_2) > 95% as measured by pulse oximetry on the hindlimb (MouseOx®, Starr Life Sciences Corp). To avoid the initial hyperglycaemia spike evoked by anaesthesia, spreading depolarization experiments were conducted > 30 min after anaesthesia induction. *In vivo* cortical spreading depolarization threshold was determined by sequential application of KCl (125, 250, 500, 1000 mM, 2 μl) directly applied to the pial surface within the cranial window, as described previously.[8] Spreading depolarization was detected electrophysiologically by a strong negative DC shift and an IOS signal (> 640 nm light scatter) recorded with a CCD camera (DMK27BU, Imaging Source).

Chronic cortical spreading depolarization monitoring in freely behaving mice

Spontaneous unfiltered cortical EEG activity was recorded with chronic electrodes implanted in freely moving Kcnq2-cKO ($Emx1^{+/cre}$-$Kcnq2^{flox/flox}$), and wild-type ($Emx1^{+/+}$-$Kcnq2^{flox/flox}$) mice. Juvenile mice [postnatal Day (P)18–20, 12–18 g body weight] were anaesthetized with isofluorane (3% induction, 1.5–2.0% maintenance), scalp hair removed, and the skin cleansed with iodine/70% ethanol, locally anaesthetized by lidocaine/bupivacaine mix, and a midline incision was made to expose the skull. Four bilaterally symmetric burr holes were made (±2 mm lateral, ±1.5 mm anterior/posterior) over the frontal and parietal cerebral surface, and two burr holes for ground electrodes over the cerebellum (±1 mm lateral, +1 mm posterior from lambda). Silicon-coated silver wires (0.5 mm diameter) were inserted into the subdural space. A

microconnector connected to the leads was glued onto the skull and cemented using Metabond (Parkell Inc). After recovery, mice were injected with meloxicam (5 mg/kg, subcutaneous) for 3 days for postoperative analgesia. Recordings were started as early as 5 days after surgery. Mice were transferred to a transparent box and the implanted microconnectors were tethered to the DC amplifier (ADI bioamp). DC activity was chronically monitored using ADI Powerlab software system. The recording room was maintained on a 12-h dark-light cycle. Mice were able to freely explore and had access to water and food. A seizure was identified as a slow stereotypic sharp wave oscillation overriding a small DC shift (~0.2 mV) while spreading depolarization was detected as a negative DC shift >5 mV in peak amplitude and the depolarization lasting for at least 30 s.

Drugs

Retigabine was obtained from Tocris and ML213 from Sigma. Both drugs were freshly dissolved in dimethyl sulphoxide (DMSO) at 100 mM on the day of the experiment. XE991 was purchased from Alomone labs and Sigma.

Data availability

Data supporting the findings of this study are available within the article and upon request.

Results

Spontaneous cortical spreading depolarization in awake Kcnq2-cKO mice

We first characterized spontaneous spreading depolarization generation in Kcnq2-deficient mice using chronic DC-band EEG recordings in awake animals implanted with cortical surface EEG electrodes. Because homozygous *Kcnq2* deletion in the germline (Sox2-cre[43]) and pan-neuronal (Actl6b-cre[44]) population resulted in neonatal death (at P0–1), likely due to respiratory failure,[45] we studied conditional *Kcnq2* KO (Emx1-cre::Kcnq2$^{flox/flox}$, hereafter Kcnq2-cKO) mice in which *Kcnq2* is selectively deleted in forebrain excitatory cells as well as peripheral ganglia,[46] allowing prolonged survival into adulthood. To capture the native early developmental epilepsy phenotype while minimizing post-surgical mortality, the bilateral cortical EEG electrodes were implanted in P19–22 mice (Fig. 1A) and recordings were conducted >5 days after surgical recovery.

By optimizing the recording conditions, we obtained stable DC-band EEG recordings in freely behaving mice sufficient to detect sub-millivolt slow DC potential changes over multiple days of monitoring. During the chronic recording, we identified stereotyped large negative DC shifts, suggestive of spreading depolarization, in association with generalized cortical seizure activity (Fig. 1B and C). During a total of >1500 h of chronic recordings from six Kcnq2-cKO mice, we detected 35 discrete spreading depolarizations in the aftermath of seizure activity (0.6 ± 0.4 spreading depolarization per day, $n = 8$ mice, total 67 days monitoring). The spontaneous seizure and spreading depolarization events were tightly coupled; 97% (34/35) of seizures were followed by spreading depolarization, and all spreading depolarizations were preceded by seizure activity (Fig. 1E). The spreading depolarization generation pattern was regionally stereotyped, in that spreading depolarizations were always first detected in the posterior cortex and were bilaterally synchronous (left versus right offset: 2.5 ± 3.6 s). The mean duration of seizure events was 23.4 ± 8.7 s, and the duration of the DC shift was 118 ± 51 s (anterior) and 100 ± 40 s (posterior). The mean spreading depolarization amplitude was larger in posterior (13.3 ± 3.9 mV) than anterior (8.4 ± 3.1 mV) electrodes ($P < 0.001$). Spreading depolarization propagation velocity (calculated based on the distance between posterior and anterior electrode pairs) was 8.4 ± 10.9 mm/min. This high velocity is consistent with the fast spreading depolarization propagation rate in Kcnq2-cKO cortical slices (discussed later in Fig. 4E and F); however, spatial variability in spreading depolarization generation/propagation pattern (e.g. generation between electrodes) may also contribute to the calculated velocity.

Following recovery from the large bilateral negative shift, unilateral ectopic slow DC shifts were occasionally detected at a posterior electrode (Fig. 1C, red arrow), possibly representing a new isolated spreading depolarization event or redetection of a wandering spreading depolarization. Thus, unlike the stereotypic spreading depolarization generation (i.e. bilateral, posterior origin), the propagation pattern of each spreading depolarization was somewhat variable. Two of the recorded mice died suddenly following a seizure-induced terminal spreading depolarization with hind-limb extension, suggestive of SUDEP.

The spectral frequencies of fast cortical EEG activity during spreading depolarization were analysed in high-pass filtered (>0.1 Hz) traces (Fig. 1D). Electrographic seizures were characterized by synchronous high amplitude oscillatory activity [Fig. 1D(b), ictal], followed by a second period of brief EEG suppression during the negative slope of the DC shift. During the nadir of the negative DC shift, fast activity was enhanced, but after recovery from the negative DC shift, EEG activity was attenuated, while small spike and burst activities were detected [Fig. 1D(c), post-spreading depolarization]. The ectopic DC shift reactivated the EEG activity even during the post-spreading depolarization EEG suppression (Fig. 1D, left, arrowhead). Video monitoring demonstrated that the initial seizure was convulsive, followed by post-ictal immobility during the spreading depolarization phase. Overall, a single seizure led to a complex EEG and behaviour abnormality sequence lasting 1–3 min in these animals.

No seizure or spreading depolarization was ever detected in paired littermate wild-type control mice. In prolonged circadian recordings, we also found that 80% (28/35) of seizure-spreading depolarization events in the mutants were detected during the dark phase, suggesting an influence of diurnal rhythm (Fig. 1F). Together, chronic DC recordings revealed a unique aspect of the epileptic phenotype of Kcnq2-cKO mice characterized by tight seizure-spreading depolarization coupling, bilateral spreading depolarization generation/propagation, and a strong diurnal expression.

Spontaneous seizure and spreading depolarization in K_v1.1-KO mice

To compare the role of epilepsy-related potassium currents in spreading depolarization, we made similar chronic recordings from age-matched juvenile *Kcna1* knockout mice. *Kcna1* encodes K_v1.1, a tetrameric voltage-gated potassium channel mediating delayed rectifier current widely expressed in the brain. Similar to Kcnq2, K_v1.1 is enriched within the axonal initial segment,[47,48] and loss of these channels results in severe epilepsy in fly, mice, and humans.[49–53] The seizure phenotype in K_v1.1-KO mice is well documented; however, *in vivo* cortical spreading depolarization susceptibility in this model has not been studied.

In chronic recordings from eight K_v1.1 KO mice (P30–40), we identified 166 seizures (3.8 ± 5.0 per day) and 23 spreading depolarization episodes (0.3 ± 0.2 per day) over 43 days of recording. Unlike Kcnq2-cKO mice, the co-occurrence of seizure and spreading depolarization was far less common; of 166 seizures detected, only

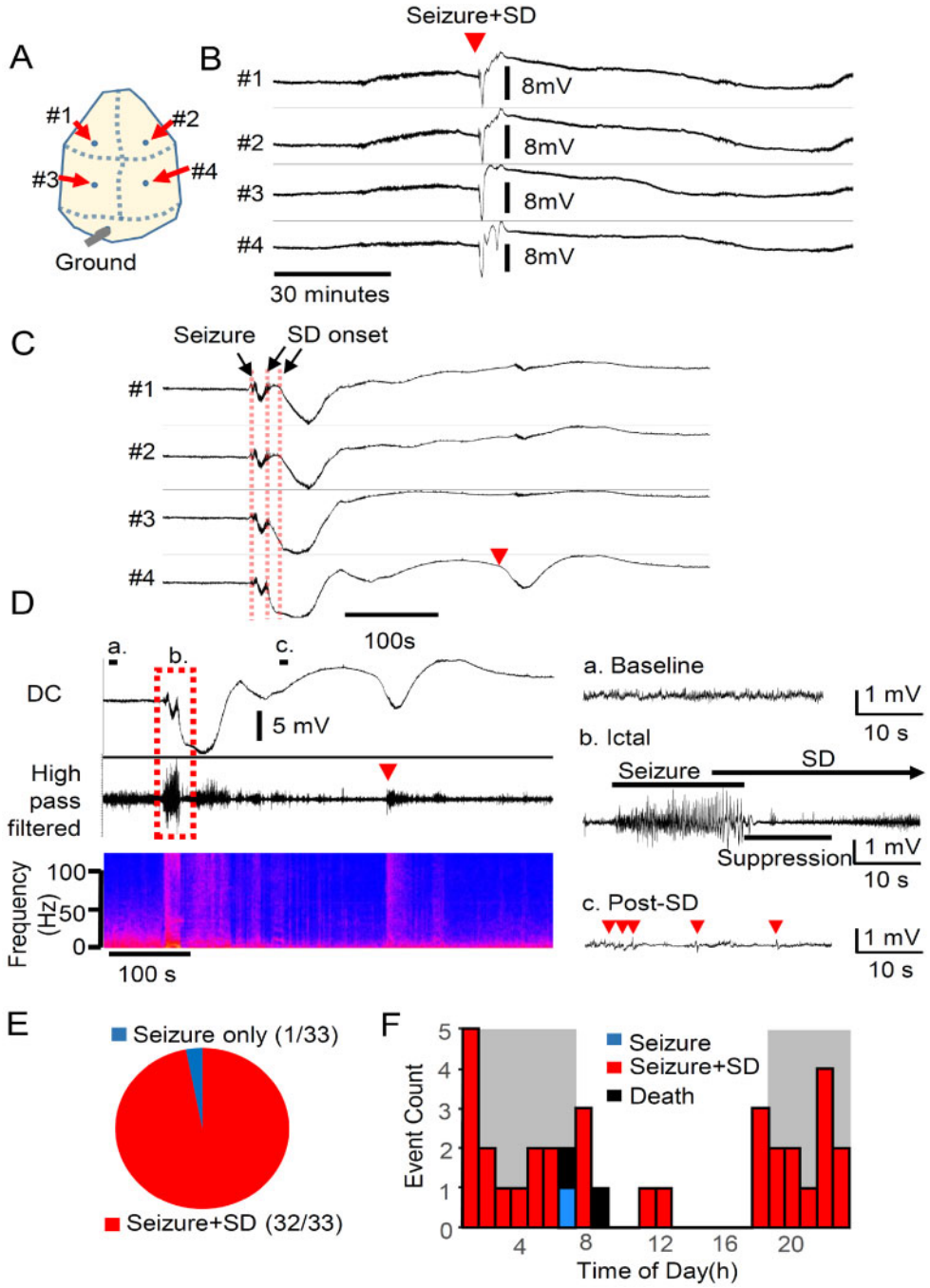

Figure 1 Spontaneous seizure/spreading depolarization complexes predominate in Emx1-Kcnq2cKO mice. Chronic cortical DC recording from juvenile Kcnq2-cKO mouse. (**A**) Recording configuration. (**B** and **C**) Spontaneous seizure/spreading depolarization complex in awake Kcnq2-cKO mouse shown at slow (**B**) and fast (**C**) time scales. Spreading depolarization was detected as a sharp negative DC potential shift following a brief generalized seizure detected simultaneously in both hemispheres. A solitary ectopic DC shift was occasionally detected posteriorly (**C**, arrowhead). (**D**) Characterization of fast EEG activity during seizure and spreading depolarization. The negative DC shifts of spreading depolarization were detected immediately after or even before the end of seizure activity. *Left*: Slow time scale. *Right*: Faster scale. High frequency EEG activity was enhanced during the nadir of the DC shift (b), followed by suppression with occasional spikelets (c). (**E**) Almost all (97%, n = 34/35) spontaneous seizures were followed by spreading depolarization. No spreading depolarizations were detected without a preceding seizure. (**F**) Circadian cycle of seizure/spreading depolarization complexes in seven Kcnq2-cKO mice. Histogram of seizure and spreading depolarization incidence during 24 h period (bin size = 1 h, dark grey = dark phase). Spontaneous seizure/spreading depolarization complexes were detected primarily during the dark phase ($P < 0.0001$, Fisher's exact test). SD = spreading depolarization.

4.8% (9/166) were associated with spreading depolarization, and 14 spreading depolarization episodes were detected without any preceding seizure activity (Fig. 2A–F). The mean seizure duration was 52.1 ± 29.2 s, which is significantly longer than those detected in Kcnq2-cKO mice (Kcnq2-cKO: n = 32, K_v1.1 KO: n = 166, $P < 0.0001$, Mann Whitney U-test). In K_v1.1-KO mice, the mean durations of spreading depolarization were 97.52 ± 44.6 s (anterior) and 82.17 ± 27.0 s (posterior), and the amplitudes were 8.9 ± 5.4 mV

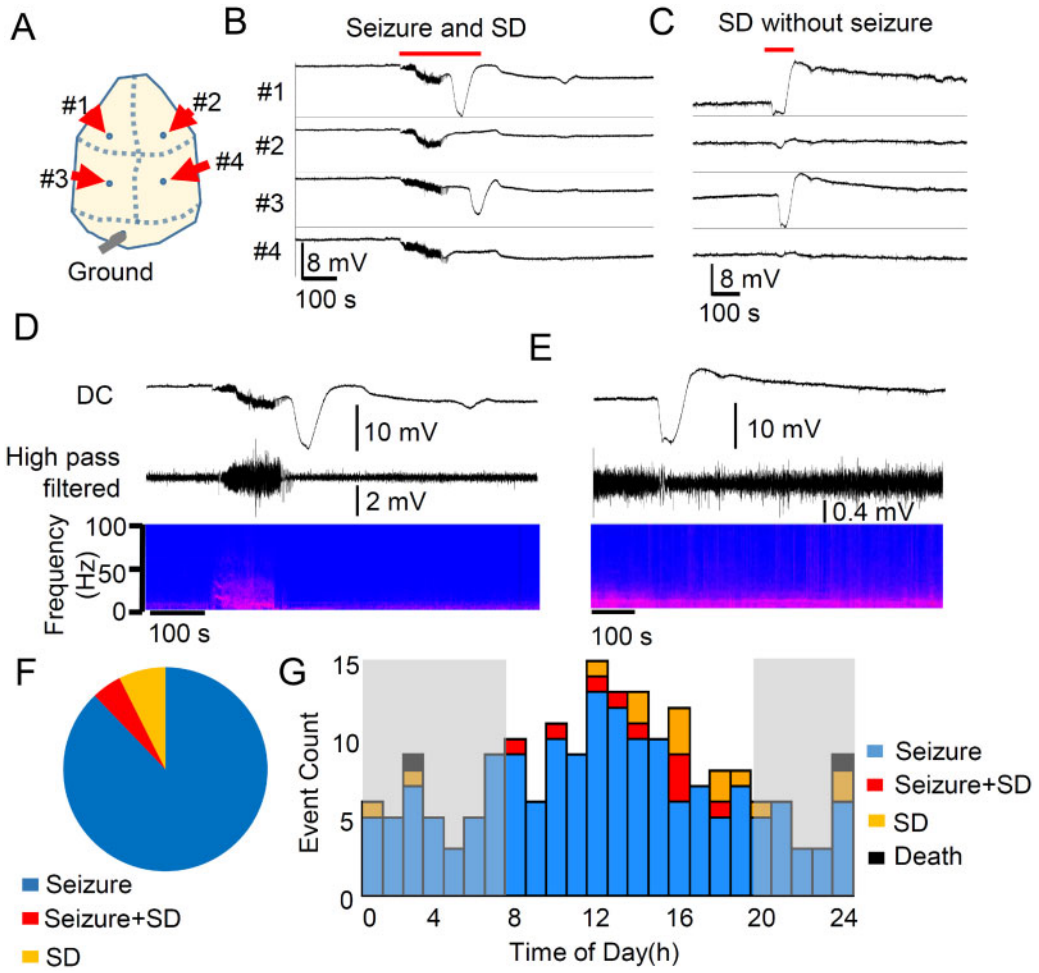

Figure 2 Spontaneous bilateral seizure with unilateral spreading depolarization and seizure independent spreading depolarization in *Kcna1* KO mice. Chronic DC recording in juvenile $K_v1.1$/Kcna1 KO mice. (**A**) Representative trace of spreading depolarization following a seizure (postictal spreading depolarization, **B**) and isolated unilateral spreading depolarization (**C**). (**D** and **E**) EEG characteristics of spreading depolarizations. No clear EEG suppression was detected in these recordings. (**F**) Unlike Kcnq2-cKO mice, seizure (n = 166) and spreading depolarization (n = 14) were often detected independently, and a seizure + spreading depolarization (SD) complex accounted for 4.8% (9/189) of total events. (**G**) Histogram of seizure, spreading depolarization, and seizure + spreading depolarization detected from eight $K_v1.1$ KO mice. There was no clear circadian dependency.

(anterior) and 7.2 ± 5.3 mV (posterior). The calculated mean spreading depolarization propagation velocity was 3.2 ± 2.5 mm/min, which is much slower than in Kcnq2-cKO ($P < 0.001$, Mann Whitney U-test). Remarkably, all nine postictal spreading depolarizations were generated following a complete termination of seizure activity with a variable mean latency (24 ± 24 s), in contrast to Kcnq2-cKO mice, in which spreading depolarizations were generated before full termination of the ongoing seizure activity.

As shown in Fig. 2B and C, 74% (17/23) of spontaneous spreading depolarization events in $K_v1.1$-KO mice were unilaterally generated even when detected following a bilateral (i.e. generalized) seizure. Thirteen per cent (3/23) of the spreading depolarization events were near-simultaneously detected in both hemispheres with a mean latency of 18.6 ± 1.6 s, whereas this latency is still much longer than that seen in Kcnq2-cKO mice (2.5 ± 3.6 s). Unlike Kcnq2-cKO mice, in $K_v1.1$-KO mice, 87% (20/23) of spreading depolarizations were detected first in the anterior electrodes (Fig. 2B and C). There was slight EEG suppression following the spreading depolarization (Fig. 2D and E), which was less pronounced compared with those reported previously in anaesthetized animals. Also, unlike the cKO model, no clear circadian dependency was detected (Fig. 2G).

Together these results indicate that the susceptibility of cortical spreading depolarization is strongly linked to intrinsic membrane excitability characteristics regulated by $K_v7.2$ and $K_v1.1$ voltage-gated potassium channels, while their regional and temporal thresholds are largely dependent on the specific channel subtype.

Kcnq/K_v7 channel inhibition in $K_v1.1$-KO mice partially phenocopies spreading depolarization pattern of Kcnq2-cKO mice

The spreading depolarization pattern in Kcnq2-cKO cortex is unusual in that these events are tightly linked to preceding seizures and are generated bilaterally. To test whether a loss of K_v7 current directly contributed to the spreading depolarization generation pattern, we administered the non-selective K_v7/Kcnq inhibitor XE991 (5–10 mg/kg, i.p.) to five $K_v1.1$-KO mice and monitored spontaneous cortical EEG activity. In all $K_v1.1$-KO mice, bilateral seizure-spreading depolarization complexes were triggered shortly after drug injection (9.9 ± 3.9 min). Three of these mice showed almost identical short-latency bilateral spreading depolarization temporal onset, while the other two showed a delayed onset (33.0

and 13.3 s) between hemispheres. The calculated spreading depolarization propagation rate of the spreading depolarizations generated following XE991 administration was faster than the spontaneous spreading depolarizations of untreated K_v1.1-KO (after XE991: 6.4 ± 2.3 mm/min, $n = 5$, spontaneous spreading depolarization: 3.2 ± 2.5 mm/min, $n = 20$; $P = 0.0041$ Mann Whitney U-test).

While cortical spreading depolarization did not provoke noticeable motor behaviour in either model, unlike the spontaneous seizure/spreading depolarization complex in Kcnq2-cKO mice, the XE991-induced seizure-spreading depolarization complex was lethal in K_v1.1-KO mice. We found that K_v1.1-KO mice barely survived the spreading depolarization and subsequently died with a latency of 5.2 ± 0.9 min (Fig. 3A), and the other two K_v1.1-KO mice died suddenly during the repolarization phase of the DC shifts (Fig. 3A, death was determined by the irreversible loss of spontaneous EEG activity). It is noteworthy that three of these K_v1.1-KO mice displayed seizures but never postictal spreading depolarization during >48-h untreated pre-drug baseline recordings, suggesting that pharmacological K_v7 inhibition not only reproduced the bilateral spreading depolarization generation pattern of Kcnq2 mutants but also facilitated postictal spreading depolarization generation. No seizures or spreading depolarization were detected in wild-type mice following XE991 administration within 24 h ($n = 4$, Fig. 3C), suggesting the drug had no proconvulsant or spreading depolarization triggering effects.

Together, these DC recording studies in awake epileptic mice suggest a critical functional role of K_v7.2 current in regulating bilateral spreading depolarization generation, and a distinctive spreading depolarization phenotype between Kcnq2 and Kcna1 mutants.

Spreading depolarization threshold is lowered in Kcnq2-cKO cortical slices *in vitro*

We next examined whether the spreading depolarization threshold of cortical networks is intrinsically altered in cortical brain slices.

The first set of experiments examined spreading depolarization generation using a seizure induction model. Cortical slices were incubated in nominally Mg^{2+}-free solution to increase spontaneous tissue excitability while monitoring local field potentials and the IOS. This condition produced spontaneous spreading depolarization following a brief episode of fast activity in both wild-type and mutant cortex. The latency until spreading depolarization onset was significantly faster in the cKO than wild-type ($P < 0.001$). With this global increase in cellular excitability, we found that spreading depolarizations were generated in multiple confluent foci, and we could not reliably calculate a propagation rate. These results indicate that the Kcnq2-cKO cortical slice is intrinsically more susceptible to spreading depolarization generation under pro-epileptic conditions.

One mechanism underlying the higher spreading depolarization susceptibility could be attributable to altered sensitivity to extracellular K^+. Therefore, we next determined the K^+ contribution to spreading depolarization threshold under physiological conditions by incrementally elevating the bath K^+ concentrations while monitoring spreading depolarization incidence as described above. These experiments revealed a subtle but significant reduction of the K^+ threshold in the cKO cortical slices (Fig. 4C and D; $P < 0.05$).

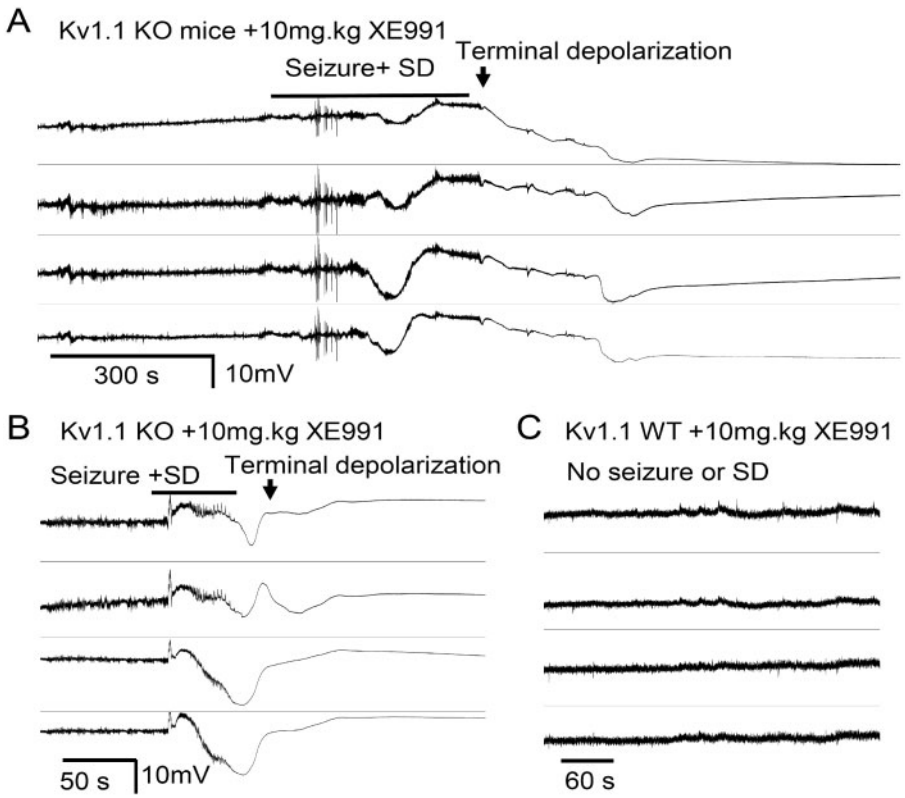

Figure 3 K_v7 inhibitor XE991 triggers bilateral seizure/spreading depolarization complex and death in K_v1.1 KO mice. After baseline recordings, K_v1.1 KO ($n = 5$) and wild-type (WT, $n = 4$) mice were administered a single dose of XE991 (5–10 mg/kg i.p.), triggering bilateral seizure-spreading depolarization complexes in all K_v1.1 KO mice. (**A**) 60% (3/5) of KO mice acutely survived the seizure-spreading depolarization complex but subsequently died. (**B**) Remaining mice (2/5) died immediately following the bilateral seizure-spreading depolarization. No seizure or spreading depolarization (SD) were detected in four K_v1.1 wild-type control mice and all survived.

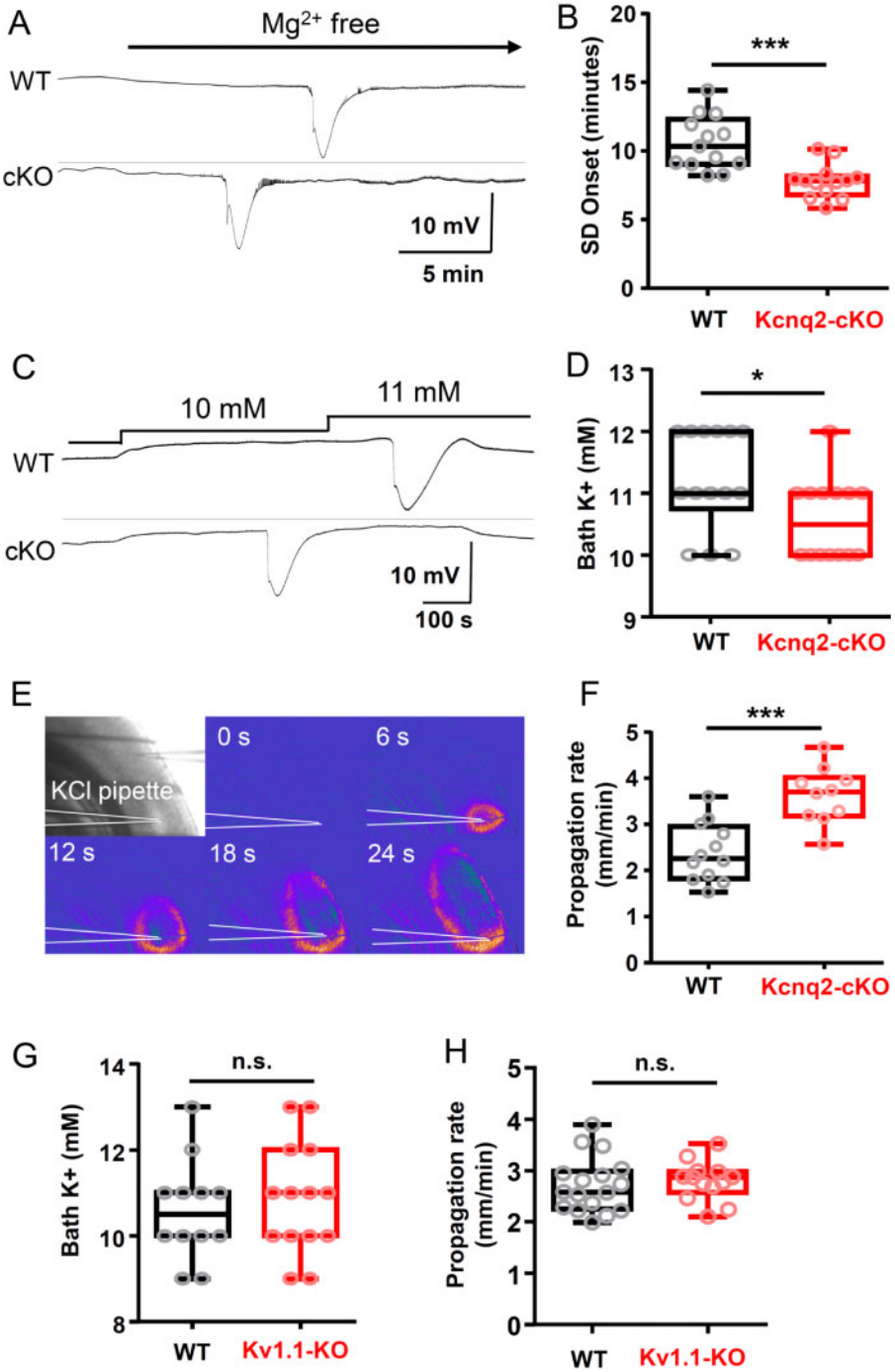

Figure 4 Spreading depolarization threshold is lowered in Kcnq2-cKO, but not in $K_v1.1$ KO cortical slices *in vitro*. (**A** and **B**) Spreading depolarization (SD) onset following exposure to nominally Mg^{2+}-free solution is faster in cKO mouse cortical slices. Representative traces (**A**) and quantification (**B**) of wild-type (WT: 10.6 ± 2.0 min, n = 13), and mutant (cKO: 7.7 ± 1.2 min, n = 12) slices. (**C** and **D**) Kcnq2-cKO cortical slices had a lowered K^+ spreading depolarization threshold. Pairs of slices were incubated and bath K^+ concentration was incrementally elevated until spreading depolarization is detected. Spreading depolarization was evoked at lower bath K^+ concentration in Kcnq2-cKO (10.6 ± 0.2 mM, n = 14) than wild-type slices (11.2 ± 0.2 mM, n = 14), $P < 0.05$. (**E** and **F**) Spreading depolarization propagation rate was faster in Kcnq2-cKO slices. Spreading depolarization was evoked by focal KCl microinjection and detected by IOS (see 'Materials and methods' section). The velocity of spreading depolarization propagation was faster in the Kcnq2-cKO slices (WT: 2.4 ± 0.2 mm/min, n = 12; cKO: 3.6 ± 0.2 mm/min, n = 10, $P < 0.005$). (**G**) Spreading depolarization threshold determined by incrementally increasing bath K^+ concentrations. (WT: 10.6 ± 0.3 mM, n = 12; KO: 10.9 ± 0.5 mM, n = 14). (**H**) Spreading depolarization propagation rate was determined by focal KCl microinjection (WT: 2.7 ± 0.1 mm/min, n = 17; KO: 2.8 ± 0.1 mm/min, n = 13). *$P < 0.05$, ***$P < 0.005$.

We also examined whether spreading depolarization propagation is altered in cKO tissue using KCl microinjection model where, unlike the bath application model, a focally generated spreading depolarization propagates through non-depolarized cortical tissue. In these experiments, spreading depolarization was triggered by KCl microinjection (1 M KCl, 50 psi) into layer 2/3 and the propagation rate was visually analysed by tracking the IOS in an area >500 μm away from the KCl injection site (Fig. 4E) where the

arrival of IOS coincided with the DC potential shift (Fig. 4F). In agreement with the lower KCl spreading depolarization threshold, we found that spreading depolarization propagation speed was also faster in mutant cortical slices compared with the littermate control ($P < 0.005$).

We also measured spreading depolarization susceptibility of K_V1.1-WT and -KO cortical tissues prepared from P30–40 mouse pairs. Unlike Kcnq2-cKO tissue, there were no differences in spreading depolarization thresholds, as determined by K^+ bath application (Fig. 4G) or the propagation rates, as determined by KCl microinjection model (Fig. 4H).

Together, these results indicate that genetic deficiency of K_V7.2, but not K_V1.1 containing channels significantly increases intrinsic susceptibility to spreading depolarization. These different effects likely contribute to the seizure-spreading depolarization transition and unique spreading depolarization propagation pattern manifested *in vivo* in genetically and pharmacologically K_V7.2 depleted cortex.

Cortical synaptic excitatory-inhibitory balance did not correlate with spreading depolarization threshold

We examined the synaptic excitatory/inhibitory balance because a shift in this ratio has correlated with a lowered spreading depolarization threshold in some genetic mouse models.[8,54] Both the sEPSC and sIPSC amplitudes in the somatosensory layer 2/3 pyramidal neurons were increased in Kcnq2-cKO mice (Fig. 5C), while, unexpectedly, only sEPSC amplitudes were enhanced in the K_V1.1-KO neurons (Fig. 5D). There were no significant differences in the frequencies of sEPSC and sIPSC events of both epilepsy mouse mutants compared to wild-type (Fig. 5E and F). Overall, the excitatory/inhibitory balance shifted towards excitation in the global K_V1.1-KO mice, while both synaptic activities were enhanced in the interneuron-sparing Kcnq2-cKO mice. While these models are not fully comparable, each of the two potassium channel deficiencies modulates the amplitude of the resting excitatory synaptic activities, and therefore this parameter does not explain the distinct spreading depolarization threshold.

Effect of pharmacological inhibition and activation of K_V7 currents on spreading depolarization *in vitro*

We next examined the acute modulatory activities of K_V7 channel blockade or activation on spreading depolarization studied *in vitro* using XE991, a K_V7 inhibitor, and retigabine, a Kcnq2 opener. The effects on spreading depolarization propagation rate were measured using the KCl microinjection model described above (Fig. 4), in which spreading depolarization was repetitively generated in wild-type cortical slices (by KCl puffs) while incubated with vehicle (0.1% DMSO) or XE991 (50 μM, a dose expected to fully inhibit K_V7.2 containing channels[55]), followed by washout. XE991 did not modulate spreading depolarization propagation rate ($P = 0.37$, Fig. 6A). In contrast, XE991 slightly reduced the KCl threshold when examined using the KCl bath application model ($P < 0.005$, Fig. 6B). Taken together, this K_V7 inhibitor has a marginal facilitatory effect on spreading depolarization generation *in vitro*.

We then examined the effect of retigabine, a clinically used non-selective K_V7 current activator[56] (Fig. 6B and C). Retigabine was without effect at 10 μM, while at 30 μM, retigabine either completely blocked spreading depolarization (2/6 slices) or greatly reduced the speed of propagation (4/6 slices). This inhibitory effect was fully reversed by extensive drug washout (>30 min). Retigabine also elevated the KCl threshold of spreading depolarization, as measured in the incremental KCl bath application model ($P = 0.016$, Fig. 6D).

The retigabine effect is largely due to the modulation of the K_V7 channels since the inhibitory effect was absent when tested on Kcnq2-cKO brain slices (Fig. 6E). ML216, a structural analogue of retigabine and a more selective K_V7.2 and 7.4 channel opener,[57] also fully inhibited spreading depolarization generation in 80% (4/5) of experiments and reduced spreading depolarization propagation in the rest (Fig. 6F).

In addition to K_V7 channels, retigabine has an off-target potentiating effect on $GABA_A$R currents.[58,59] We therefore examined the $GABA_A$R dependency of retigabine using repetitive KCl evoked spreading depolarization in acute wild-type cortical slices. Consistent with previous studies, exposure to the $GABA_A$R antagonist, gabazine (10 μM) significantly increased the spreading depolarization propagation rate ($P < 0.05$). Retigabine was still effective in this condition, consistently reducing spreading depolarization velocity ($P < 0.01$), and the effect was reversible ($P < 0.05$). These results indicate that spreading depolarization inhibition by retigabine is independent of $GABA_A$R signalling (Fig. 6G).

The spreading depolarization inhibitory effect of retigabine was further tested in mouse cortex *in vivo*. In urethane anaesthetized wild-type adult mice, spreading depolarization was elicited by superfusing incrementally increasing concentrations of KCl onto the pial surface through a cranial window created over the posterior cortex and detected with both a surface electrode as well as transcranial imaging of the intrinsic optical signal (light scatter, Fig. 7A). In each animal, the spreading depolarization threshold was determined twice, first at pre-drug baseline, and then 20 min after intraperitoneal injection of drug or DMSO vehicle control. In these experiments, 30 mg/kg retigabine (but not 10 mg/kg) significantly increased the KCl threshold of spreading depolarization required to trigger a spreading depolarization (Fig. 7B and C).

After testing the spreading depolarization threshold, the frequency of recurrent spreading depolarization generation during a continuous 0.5 M KCl application was determined in a subset of animals. Consistent with an elevated spreading depolarization threshold, the number of recurrent spreading depolarizations in response to a continuous surface application of 0.5 M KCl was decreased following retigabine treatment (Fig. 7D).

Together these results indicate that K_V7 inhibition and activation bidirectionally modulate spreading depolarization in the wild-type brain. Given the pharmacological concentration range of retigabine on Kcnq current (0.1–100 μM[60]), these data also suggest that spreading depolarization inhibition required near-maximal concentrations for an anti-spreading depolarization effect.

Retigabine inhibits spreading depolarization in mild, but not severe OGD model

K_V7 activators have been shown to reduce neuronal damage following experimental ischaemia, where spreading depolarization could potentially contribute to progression of the lesion.[61,62] We examined whether the K_V7 activator retigabine can also inhibit spreading depolarization generated during the experimental *in vitro* ischaemia model. In this model, exposure to OGD solution (0% O_2, 0 or 2 mM glucose) results in spontaneous spreading depolarization generation (Fig. 8A and B), and the latency to the first spreading depolarization after OGD exposure is used as a readout of spreading depolarization threshold. In this model, retigabine (30 μM) was without effect when spreading depolarization was triggered by exposures to a 0% O_2/0 mM glucose solution (Fig. 8C). However, retigabine significantly delayed spreading depolarization onset when bathed with 0% O_2/2 mM glucose OGD solution

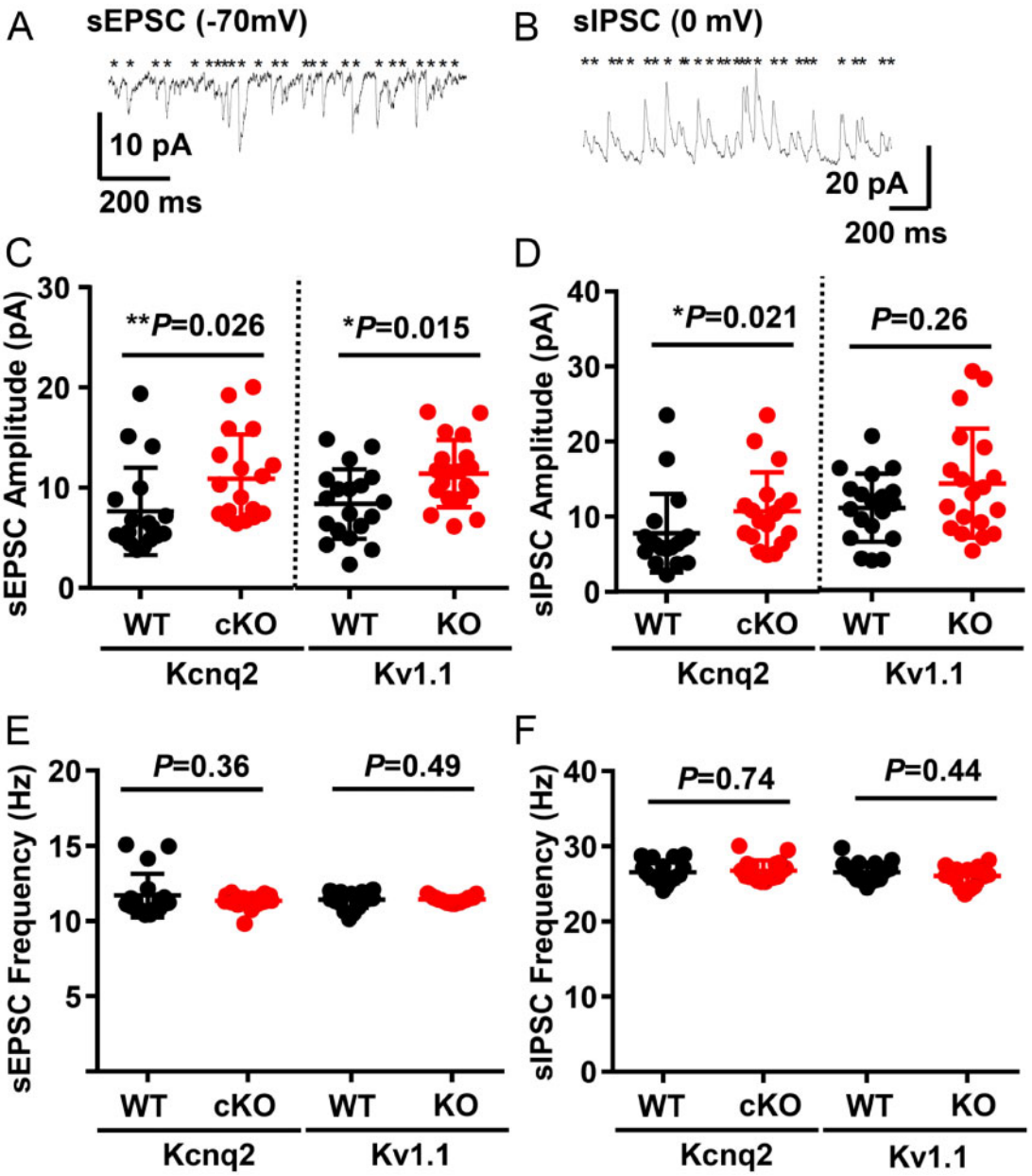

Figure 5 sEPSC and sIPSC balances in the cortical layer 2/3 pyramidal neurons of Kcnq2-cKO and K_v1.1-KO mice. (**A** and **B**) Representative traces of sEPSC and sIPSC activity recorded from layer 2/3 cortical pyramidal neurons. (**C** and **D**) SEPSC amplitudes were enhanced in both Kcnq2-cKO [wild-type (WT): 7.6 ± 1.0 pA; cKO: 10.9 ± 1.0pA) and K_v1.1-KO (WT: 8.4 ± 0.8 pA; KO: 11.40 ± 0.8pA), while sIPSC amplitudes were increased only in Kcnq2-cKO (WT: 7.8 ± 1.2 pA; cKO: 10.7 ± 1.2pA), not in K_v1.1-KO cortical tissue (WT: 11.0 ± 1.0 pA; KO: 14.2 ± 1.7 pA). (**E** and **F**) No differences were detected in the frequencies of sEPSC (Kcnq2-WT: 23.2 ± 0.7 Hz, -cKO: 22.7 ± 0.2 Hz; K_v1.1-WT: 22.7 ± 0.3 Hz, -KO: 22.9 ± 0.1 Hz) and sIPSC (Kcnq2-WT: 26.8 ± 0.3 Hz, -cKO: 27.0 ± 0.4 Hz, K_v1.1-WT: 26.6 ± 0.3 Hz, -KO: 26.1 ± 0.3 Hz). n = 18 for Kcnq2-WT and cKO, n = 19 for K_v1.1 WT and KO neurons. Mann-Whitney U-test was used for the statistical comparisons of these data.

(Fig. 8C). Thus, the acute inhibitory effect of retigabine appears limited under conditions of mild hypoxic/metabolic deprivation, but not effective when glucose metabolism is severely compromised.

To determine whether retigabine might be effective in subcortical brain regions where seizure-induced spreading depolarization has been linked to local hypoxia and cardiorespiratory arrest,[7] we examined its effect on spreading depolarization evoked by OGD in slices of medulla containing the nucleus tractus solitaries (nTS). Some ion channel mutations implicated in SUDEP, including loss of K_v1.1, significantly lower spreading depolarization threshold in this region.[7,8] The effect of retigabine was tested in brainstem slices prepared from juvenile K_v1.1 KO mice based on the latency to OGD-spreading depolarization onset determined by the IOS changes (Fig. 8E–G). Retigabine did not block or delay spreading depolarization onset in this model under 5 mM glucose OGD conditions (Fig. 8G). Thus, the inhibitory effect of retigabine on spreading depolarization is model-dependent and likely influenced by both the severity of metabolic stress and the functional contribution of Kcnq2 channels in different anatomical networks.

Discussion

Our study identifies a novel role of Kcnq2/K_v7.2 in the regulation of susceptibility to pathological long-lasting depolarization of cortical networks. Chronic DC recordings in freely behaving mice revealed

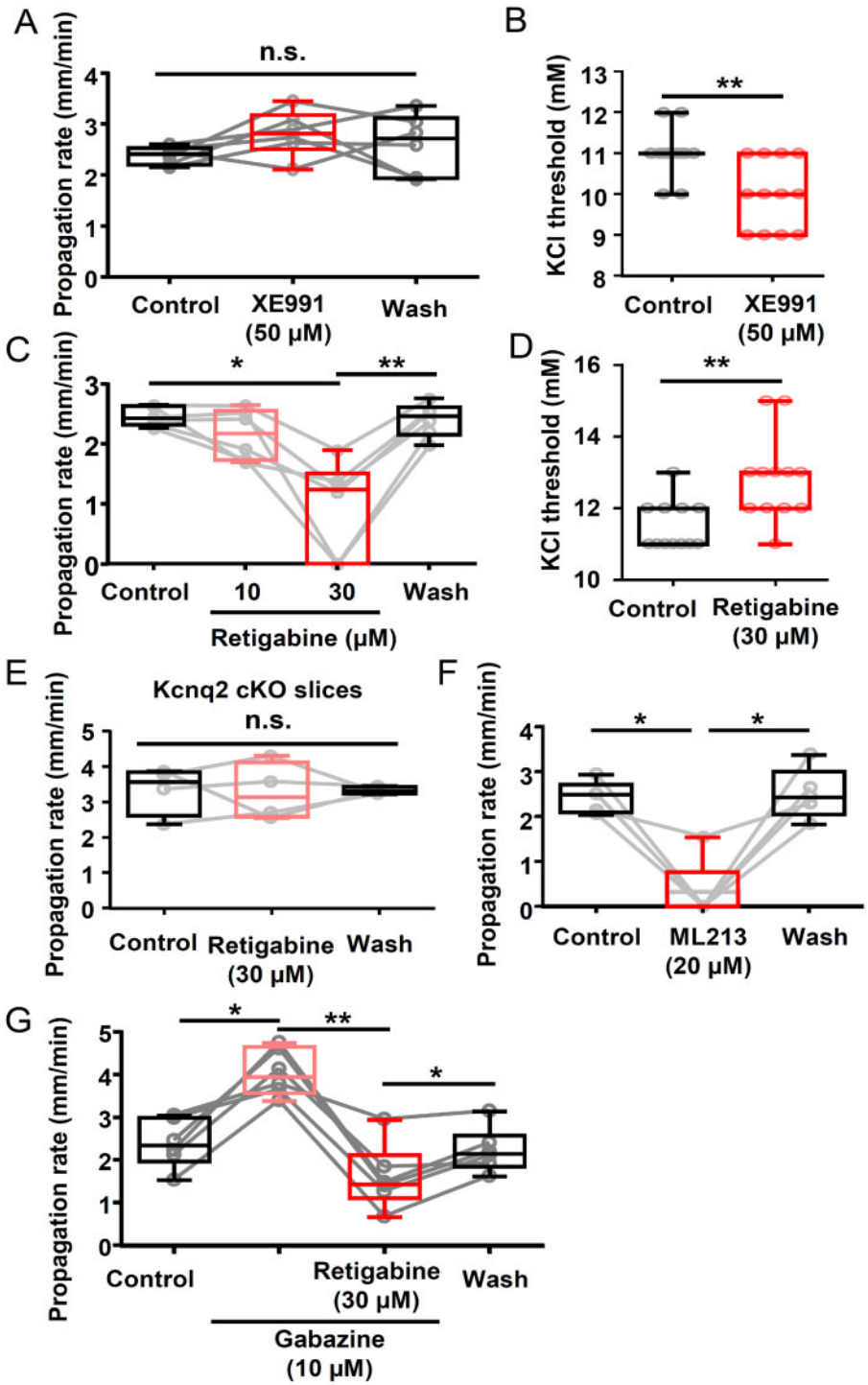

Figure 6 Acute enhancement/inhibition of spreading depolarization in wild-type cortex by K_v7 inhibitor/activator *in vitro*. (**A** and **B**) Effect of XE991 on spreading depolarization propagation rate and K^+ threshold. (**A**) Spreading depolarization propagation rate measured from spreading depolarizations repetitively generated in single slices while incubated in the drug was unchanged. Control: 2.4 ± 0.2 mm/min, XE991: 2.8 ± 0.5 mm/min, Wash: 2.6 ± 0.6 mm/min, n = 6, P = 0.37. n.s. = not significant. (**B**) Spreading depolarization threshold was decreased by Kcnq inhibitor in K^+ bath application model. Control: 11.0 ± 0.2 mM, XE991: 10.0 ± 0.2 mM, n = 12 each, $^*P < 0.005$. (**C** and **D**) Retigabine dose-dependently reduced spreading depolarization propagation rate (**C**, n = 6) and elevated the K^+ threshold (vehicle: 11.5 ± 0.2 mM, retigabine: 12.8 ± 0.3 mM, n = 12, P = 0.016) (**D**, n = 12). (**E**) Retigabine (30 μM) did not alter spreading depolarization propagation in Kcnq2-cKO slices, n = 4. (**F**) ML216 (20 μM), another K_v7 activator, also inhibited spreading depolarization propagation in wild-type slices (Control: 2.4 ± 0.4 mm/min, ML216: 0.3 ± 0.7 mm/min, wash: 2.5 ± 0.6 mm/min, n = 5). (**G**) Retigabine effect on spreading depolarization was analysed in the presence of the $GABA_AR$ antagonist gabazine. Gabazine increased the spreading depolarization propagation rate; however, retigabine still reduced the spreading depolarization propagation rate (Control: 2.4 ± 0.6 mm/min, gabazine: 4.1 ± 0.5 mm/min, gabazine + retigabine: 1.6 ± 0.8 mm/min, wash: 2.2 ± 0.5 mm/min, n = 6, $^*P < 0.05$, $^{**}P < 0.01$).

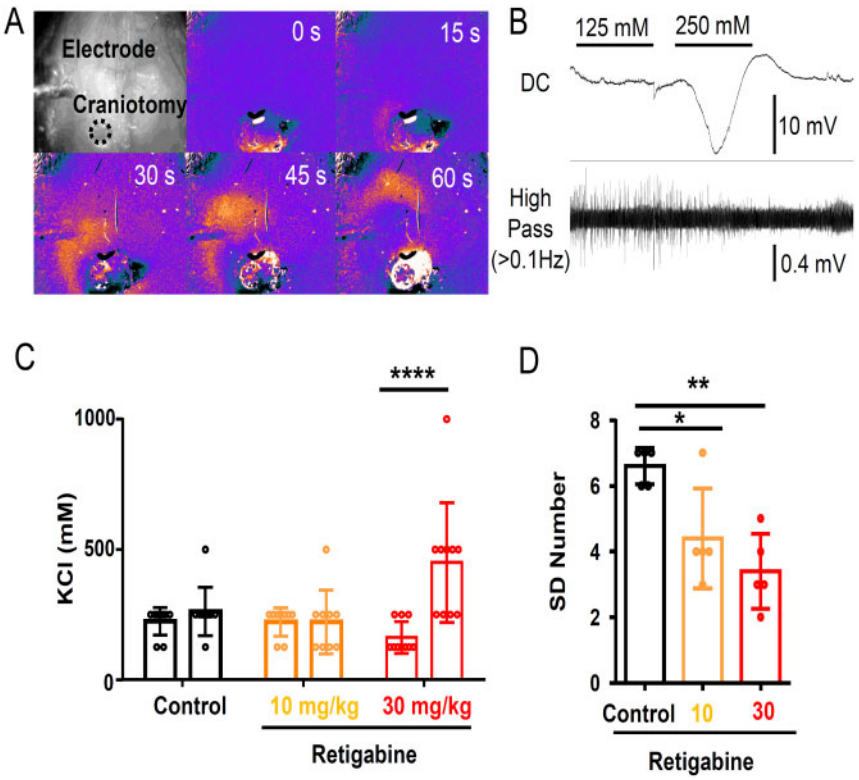

Figure 7 Spreading depolarization inhibition by retigabine in *in vivo* anaesthetized wild-type mouse cortex. Spreading depolarization was triggered by repetitively applying a KCl solution (100, 300, 500, 1000 mM for 2 min) to the cortical surface. (**A**) Spreading depolarization wave was detected with IOS signal shown in a pseudocoloured image, and (**B**) electrophysiologically with Ag/AgCl electrode. (**C**) Summary of spreading depolarization threshold measurement. In each animal, spreading depolarization threshold was measured before and after drug injection. Vehicle (0.1% DMSO) and 10 mg/kg retigabine had no effect, while 30 mg/kg retigabine significantly increased K^+ evoked spreading depolarization threshold. $^{****}P < 0.001$. (**D**) Number of recurrent spreading depolarization events during continuous 0.5 M KCl application for 30 min. Retigabine 30 mg/kg significantly decreased the regenerative spreading depolarization number. $^{*}P < 0.05$, $^{**}P < 0.01$.

a distinctive cortical spreading depolarization phenotype when $K_v7.2$ subunits are genetically removed or pharmacologically inhibited compared to a related axonal potassium channel, Kcna1/$K_v1.1$. Unlike $K_v1.1$-deficient mice, loss of $K_v7.2$ in excitatory neurons facilitated tightly coupled seizure-spreading depolarization transitions, bi-hemispheric spreading depolarization generation, and a circadian expression pattern favouring the dark cycle. *In vitro* analyses of acute cortical slices in response to multiple spreading depolarization triggers revealed that the lower spreading depolarization threshold is intrinsic to cortical tissue excitability and that $K_v7.2$ activity bidirectionally regulates K^+ spreading depolarization thresholds. These results support Kcnq2/$K_v7.2$ availability as a critical and pharmacologically accessible molecular determinant of spreading depolarization threshold and cortical distribution. Fluctuations of this current under pathological states[63–65] may contribute to spreading depolarization susceptibility, and serve as a therapeutic target in epilepsy and other neurological disorders.

Kcnq2/$K_v7.2$ regulates seizure/spreading depolarization transition

Seizures in Kcnq2 mice reliably triggered spreading depolarization expression 97% (34/35 events) of the time, and at very short latency, sometimes even commencing during the seizure. This is in sharp contrast to $K_v1.1$-KO mice, in which only 5% (9/175) of seizures were associated with spreading depolarization, with a significantly longer postictal latency. The severity of the seizure itself is unlikely to explain these differences, as seizure duration was longer in $K_v1.1$-KO mice and should create an even larger extracellular potassium surge and tissue hypoxia. Instead, the conversion of uncoupled seizure/spreading depolarization to a tightly coupled Kcnq2-cKO-like spreading depolarization phenotype by acute pharmacological inhibition (Fig. 3) indicates the presence of a functional Kcnq2/$K_v7.2$ activity-dependent threshold mechanism. While the threshold is multifactorial and state-dependent, our study suggests that reducing $K_v7.2$ current lowers the threshold for seizure to spreading depolarization transition. In addition to the spreading depolarization threshold, changes in tissue metabolism, astrocytic extracellular homeostasis, and synaptic network functions during chronic epileptic conditions may also modulate the spreading depolarization phenotype.[66,67]

Although they were rare, the presence of seizure-independent isolated spontaneous spreading depolarization events in awake $K_v1.1$ KO mice has not been previously reported (Fig. 2C). The triggering mechanism of these isolated events is not known, but may reflect focal changes in cortical hyperexcitation[31] or vascular insufficiency, since cerebral autoregulation may be impaired in some forms of epilepsy.[68,69]

Kcnq2/$K_v7.2$ regulation of bi-hemispheric spreading depolarization generation

Another salient feature of reduced $K_v7.2$ availability is the bi-hemispheric symmetry of spreading depolarization following a generalized seizure. The majority of spreading depolarization-related neurological deficits during migraine auras, such as visual scotomata and hemiplegia are unilateral.[70] Short latency, bi-hemispheric spreading depolarization generation in this model is likely a direct consequence of the preceding generalized seizure activity, which raises extracellular K^+ and lowers tissue oxygenation in both hemispheres simultaneously. A similar bilateral spreading

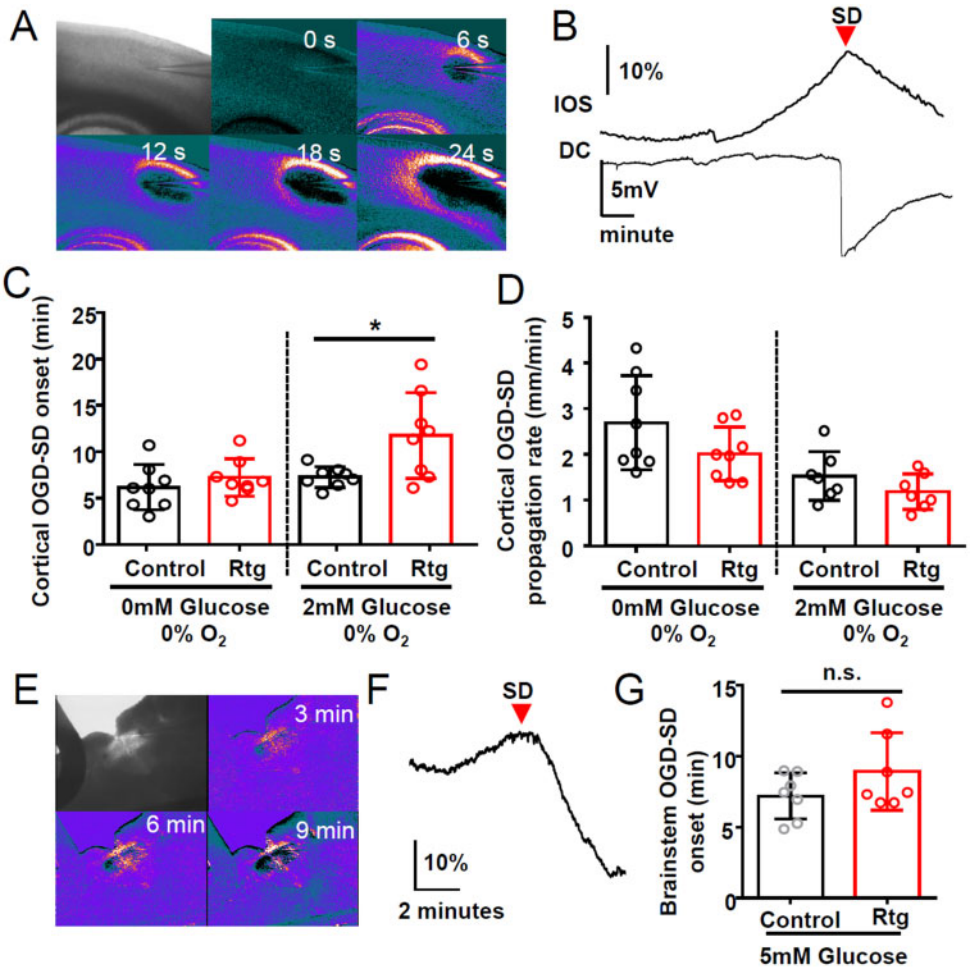

Figure 8 K_v7.2 activator retigabine inhibits mild, but not severe OGD-induced spreading depolarization. (**A**) Image of OGD-spreading depolarization wave in cortical slice triggered by continuous exposure to OGD solution (0% O_2, 0 mM glucose), and detected as IOS travelling across cortical tissue. (**B**) Arrival of IOS signal (*top*) near electrode coincided with negative DC potential shift (*bottom trace*). (**C** and **D**) Retigabine delayed OGD-spreading depolarization when metabolic stress was mild (2 mM glucose), but had no effect during severe compromise (0 mM glucose). Retigabine did not inhibit spreading depolarization propagation rate (**D**) $n = 8$ each, $^*P < 0.05$. (**E–G**) Retigabine had no effect on OGD-spreading depolarization generated in slices of the medulla at the level of the nucleus tractus solitarius (nTS). (**E**) Spreading depolarization was triggered by 0% O_2/5 mM glucose solution with or without 30 μM retigabine. (**F** and **G**) Spreading depolarization onset was determined by the IOS signal peak at the lateral margin of the nTS. ($n = 7$ in all experiments). SD = spreading depolarization.

depolarization generation has been reported following a generalized seizure induced by systemic chemoconvulsant (pentylenetetrazol) injection.[25] In this regard, the predominant unilateral spreading depolarization in K_v1.1-KO mice after a bilateral generalized seizure seems more difficult to explain (Fig. 2B); however, the fact that acute K_v7 inhibition produced bi-hemispheric spreading depolarization generation in K_v1.1 KO mice indicates that K_v7 activity acts as a barrier for bilateral generation. Based on its enrichment within axonal initial segments and nodes,[37,47] K_v7.2 activity may limit long-range (e.g. transcallosal) axonal propagation of hyperactivity, thereby reducing the likelihood of contralateral spreading depolarization generation in symmetric brain regions, as described in Leao's seminal study.[71] This mechanism might also contribute to the faster tissue propagation velocity into the surrounding neocortex.

Spreading depolarization modulation by K_v7.2 activity

Kcnq2/K_v7.2 containing channels generate a non-inactivating outward current that counteracts the generation of persistent sodium current (INaP[72]) an initial inward current of spreading depolarization.[1] Genetic deletion or pharmacological inhibition of M-current likely facilitates INaP and facilitated continuous membrane depolarization, while augmentation may attenuate INaP, which may elevate the spreading depolarization threshold. This relationship is in contrast to K_v1.1, which acts to limit action potential bandwidth and frequency.[37,52,73] Loss of this fast current may be critical for promoting synchronous action potential bursting leading to seizures, but might be less important as a brake for slow sustained cellular depolarization leading to spreading depolarization.

Both K_v1.1 and K_v7.2 regulate axonal excitability and neurotransmitter release. However, changes in the excitatory-inhibitory synaptic balance did not clearly correlate with spreading depolarization threshold. The increased sIPSC amplitude in the Kcnq2-cKO, but not in the global K_v1.1-KO, was unexpected because selective deletion of the K_v7.2 channel in excitatory neurons should not directly alter the excitability of inhibitory neurons. These lasting changes in synaptic excitatory-inhibitory balance may be due to complex remodelling and synaptic/circuit homeostasis during the formation of hyperexcitable recurrent circuitry.[66] Similar biological changes during chronic epilepsy might also affect

spreading depolarization thresholds, and we have observed elevated cortical spreading depolarization threshold in ageing $K_v1.1$ KO mice.

We showed that retigabine could delay spreading depolarization onset following submaximal OGD stimulation. Interestingly, $K_v7.2$ activators are neuroprotective in experimental ischaemia and brain trauma studies,[60,61,64,74,75] and the anti-spreading depolarization properties of the activator may contribute to these neuroprotective effects. It should be noted that only a relatively high, sedating, drug concentration effectively inhibited spreading depolarization. Thus, these activators may be of limited prophylactic utility, while they might find an adjunctive role in sedated patients requiring critical care. We also found asymmetric effects of the Kcnq2 activator and inhibitor. The K_v7 inhibitor had a relatively small facilitatory effect on spreading depolarization generation, whereas the activator could fully suppress spreading depolarization at a high concentration. This result may indicate relatively small basal K_v7 activity, with a capacity to generate larger currents upon potentiation by GPCR signalling and binding of agonists.[76,77] It has also been suggested that K_v7 activators may indirectly antagonize NMDARs, which are important contributors to spreading depolarization initiation/propagation.[78] However evidence of functional NMDAR inhibition is limited and requires further study.

While our study identifies a major role of $K_v7.2$ expressed in excitatory neurons in the regulation of spreading depolarization, their role in inhibitory neurons has not been assessed here and could also impact spreading depolarization, but likely in a more complex manner. As evident from our result (Fig. 6G), acute network disinhibition facilitates spreading depolarization and thus global Kcnq2 deficiency may have a less pronounced phenotype compared to the cKO model. On the other hand, potentiation of GABA had little spreading depolarization modulatory effect,[79] and increased interneuronal excitability by Kcnq2/$K_v7.2$ deletion may instead facilitate spreading depolarization by accelerating extracellular K^+ accumulation.[34,80] Further study is needed to fully elucidate the role of $K_v7.2$ currents in specific inhibitory interneuron populations, which may have additional significance in KCNQ2 encephalopathies.

Acknowledgement

We thank Dr A. Tzingounis for generously sharing Kcnq2-flox mice.

Funding

This work was supported by American Heart Association career development grant 19CDA34660056 (I.A.), Curtis Hankamer Basic Research Fund at Baylor College of Medicine (I.A.), NIH Center for SUDEP Research (NS090340 and NS29709, J.L.N.), and Blue Bird Circle Foundation (J.L.N.)

Competing interests

The authors report no competing interests.

References

1. Somjen GG. Mechanisms of spreading depression and hypoxic spreading depression-like depolarization. *Physiol Rev*. 2001; 81(3):1065–1096.
2. Dreier JP. The role of spreading depression, spreading depolarization and spreading ischemia in neurological disease. *Nat Med*. 2011;17(4):439–447.
3. Dreier JP, Major S, Foreman B, et al. Terminal spreading depolarization and electrical silence in death of human cerebral cortex. *Ann Neurol*. 2018;83(2):295–310.
4. Carlson AP, Shuttleworth CW, Major S, Lemale CL, Dreier JP, Hartings JA. Terminal spreading depolarizations causing electrocortical silencing prior to clinical brain death: Case report. *J Neurosurg*. 2018;131(6):1773–1779.
5. Dreier JP, Major S, Lemale CL, et al. Correlates of spreading depolarization, spreading depression, and negative ultraslow potential in epidural versus subdural electrocorticography. *Front Neurosci*. 2019;13:373.
6. Major S, Huo S, Lemale CL, et al. Direct electrophysiological evidence that spreading depolarization-induced spreading depression is the pathophysiological correlate of the migraine aura and a review of the spreading depolarization continuum of acute neuronal mass injury. *GeroSci*. 2020;42(1):57–80.
7. Aiba I, Noebels JL. Spreading depolarization in the brainstem mediates sudden cardiorespiratory arrest in mouse SUDEP models. *Sci Transl Med*. 2015;7(282):282ra46.
8. Aiba I, Wehrens XHT, Noebels JL. Leaky RyR2 channels unleash a brainstem spreading depolarization mechanism of sudden cardiac death. *Proc Natl Acad Sci U S A*. 2016;113(33):E4895–E4903.
9. Loonen ICM, Jansen NA, Cain SM, et al. Brainstem spreading depolarization and cortical dynamics during fatal seizures in *Cacna1a* S218L mice. *Brain*. 2019;142(2):412–425.
10. Hatcher A, Yu K, Meyer J, Aiba I, Deneen B, Noebels JL. Pathogenesis of peritumoral hyperexcitability in an immunocompetent CRISPR-based glioblastoma model. *J Clin Invest*. 2020; 130(5):2286–2300.
11. Dreier JP, Reiffurth C. The stroke-migraine depolarization continuum. *Neuron*. 2015;86(4):902–922.
12. Herreras O, Makarova J. Mechanisms of the negative potential associated with Leão's spreading depolarization: A history of brain electrogenesis. *J Cereb Blood Flow Metab*. 2020;40(10): 1934–1952.
13. Takizawa T, Qin T, Lopes de Morais A, et al. Non-invasively triggered spreading depolarizations induce a rapid pro-inflammatory response in cerebral cortex. *J Cereb Blood Flow Metab*. 2020; 40(5):1117–1131.
14. Harriott AM, Chung DY, Uner A, et al. Optogenetic spreading depression elicits trigeminal pain and anxiety behavior. *Ann Neurol*. 2021;89(1):99–110.
15. Gabriel S, Njunting M, Pomper JK, et al. Stimulus and potassium-induced epileptiform activity in the human dentate gyrus from patients with and without hippocampal sclerosis. *J Neurosci*. 2004;24(46):10416–10430.
16. Avoli M, Drapeau C, Louvel J, Pumain R, Olivier A, Villemure JG. Epileptiform activity induced by low extracellular magnesium in the human cortex maintained in vitro. *Ann Neurol*. 1991;30(4): 589–596.
17. Fabricius M, Fuhr S, Willumsen L, et al. Association of seizures with cortical spreading depression and peri-infarct depolarisations in the acutely injured human brain. *Clin Neurophysiol*. 2008;119(9):1973–1984.
18. Dreier JP, Major S, Pannek H-W, et al.; COSBID study group. Spreading convulsions, spreading depolarization and epileptogenesis in human cerebral cortex. *Brain J Neurol*. 2012;135(Pt 1): 259–275.
19. Wei Y, Ullah G, Schiff SJ. Unification of neuronal spikes, seizures, and spreading depression. *J Neurosci*. 2014;34(35): 11733–11743.

20. Lapilover EG, Lippmann K, Salar S, et al. Peri-infarct blood-brain barrier dysfunction facilitates induction of spreading depolarization associated with epileptiform discharges. *Neurobiol Dis*. 2012;48(3):495–506.
21. Somjen GG. Ion regulation in the brain: Implications for pathophysiology. *Neurosci Rev J*. 2002;8(3):254–267.
22. Raimondo JV, Burman RJ, Katz AA, Akerman CJ. Ion dynamics during seizures. *Front Cell Neurosci*. 2015;9:419.
23. Hablitz JJ, Heinemann U. Alterations in the microenvironment during spreading depression associated with epileptiform activity in the immature neocortex. *Brain Res Dev Brain Res*. 1989; 46(2):243–252.
24. Bogdanov VB, Middleton NA, Theriot JJ, et al. Susceptibility of primary sensory cortex to spreading depolarizations. *J Neurosci*. 2016;36(17):4733–4743.
25. Koroleva VI, Vinogradova LV, Bures J. Reduced incidence of cortical spreading depression in the course of pentylenetetrazol kindling in rats. *Brain Res*. 1993;608(1):107–114.
26. Xu S-Y, Li Z-X, Wu X-W, Li L, Li C-X. Frequency and pathophysiology of post-seizure todd's paralysis. *Med Sci Monit Int Med J Exp Clin Res*. 2020;26:e920751.
27. van den Maagdenberg AMJM, Pietrobon D, Pizzorusso T, et al. A Cacna1a knockin migraine mouse model with increased susceptibility to cortical spreading depression. *Neuron*. 2004;41(5):701–710.
28. van den Maagdenberg AMJM, Pizzorusso T, Kaja S, et al. High cortical spreading depression susceptibility and migraine-associated symptoms in Ca(v)2.1 S218L mice. *Ann Neurol*. 2010;67(1): 85–98.
29. Unekawa M, Ikeda K, Tomita Y, Kawakami K, Suzuki N. Enhanced susceptibility to cortical spreading depression in two types of Na + ,K + -ATPase α2 subunit-deficient mice as a model of familial hemiplegic migraine 2. *Cephalal Int J Headache*. 2018; 38(9):1515–1524.
30. Kros L, Lykke-Hartmann K, Khodakhah K. Increased susceptibility to cortical spreading depression and epileptiform activity in a mouse model for FHM2. *Sci Rep*. 2018;8(1):16959.
31. Parker PD, Suryavanshi P, Melone M, et al. Non-canonical glutamate signaling in a genetic model of migraine with aura. *Neuron*. 2021;109(4):611–628.e8.
32. Leo L, Gherardini L, Barone V, et al. Increased susceptibility to cortical spreading depression in the mouse model of familial hemiplegic migraine type 2. *PLoS Genet*. 2011;7(6):e1002129.
33. Jansen NA, Dehghani A, Linssen MML, Breukel C, Tolner EA, van den Maagdenberg AMJM. First FHM3 mouse model shows spontaneous cortical spreading depolarizations. *Ann Clin Transl Neurol*. 2020;7(1):132–138.
34. Chever O, Zerimech S, Scalmani P, et al. GABAergic neurons and Na V 1.1 channel hyperactivity: A novel neocortex-specific mechanism of cortical spreading depression. *bioRxiv*. [Preprint] doi:10.1101/2020.03.14.991158
35. Reiffurth C, Alam M, Zahedi-Khorasani M, Major S, Dreier JP. Na + /K + -ATPase α isoform deficiency results in distinct spreading depolarization phenotypes. *J Cereb Blood Flow Metab*. 2020; 40(3):622–638.
36. Hu W, Bean BP. Differential control of axonal and somatic resting potential by voltage-dependent conductances in cortical layer 5 pyramidal neurons. *Neuron*. 2018;97(6):1315–1326.e3.
37. Devaux JJ, Kleopa KA, Cooper EC, Scherer SS. KCNQ2 is a nodal K + channel. *J Neurosci*. 2004;24(5):1236–1244.
38. Dirkx N, Miceli F, Taglialatela M, Weckhuysen S. The Role of Kv7.2 in neurodevelopment: Insights and gaps in our understanding. *Front Physiol*. 2020;11:570588.
39. Singh NA, Charlier C, Stauffer D, et al. A novel potassium channel gene, KCNQ2, is mutated in an inherited epilepsy of newborns. *Nat Genet*. 1998;18(1):25–29.
40. Singh NA, Westenskow P, Charlier C, et al.; BFNC Physician Consortium. KCNQ2 and KCNQ3 potassium channel genes in benign familial neonatal convulsions: Expansion of the functional and mutation spectrum. *Brain J Neurol*. 2003;126(Pt 12): 2726–2737.
41. Nappi P, Miceli F, Soldovieri MV, Ambrosino P, Barrese V, Taglialatela M. Epileptic channelopathies caused by neuronal Kv7 (KCNQ) channel dysfunction. *Pflugers Arch*. 2020;472(7): 881–898.
42. Soh H, Pant R, LoTurco JJ, Tzingounis AV. Conditional deletions of epilepsy-associated KCNQ2 and KCNQ3 channels from cerebral cortex cause differential effects on neuronal excitability. *J Neurosci*. 2014;34(15):5311–5321.
43. Hayashi S, Tenzen T, McMahon AP. Maternal inheritance of Cre activity in a Sox2Cre deleter strain. *Genes N Y N 2000*. 2003;37(2): 51–53.
44. Zhan X, Cao M, Yoo AS, et al. Generation of BAF53b-Cre transgenic mice with pan-neuronal Cre activities. *Genes N Y N 2000*. 2015;53(7):440–448.
45. Watanabe H, Nagata E, Kosakai A, et al. Disruption of the epilepsy KCNQ2 gene results in neural hyperexcitability. *J Neurochem*. 2000;75(1):28–33.
46. Gorski JA, Talley T, Qiu M, Puelles L, Rubenstein JLR, Jones KR. Cortical excitatory neurons and glia, but not GABAergic neurons, are produced in the Emx1-expressing lineage. *J Neurosci*. 2002;22(15):6309–6314.
47. Lorincz A, Nusser Z. Cell-type-dependent molecular composition of the axon initial segment. *J Neurosci*. 2008;28(53): 14329–14340.
48. Vivekananda U, Novak P, Bello OD, et al. Kv1.1 channelopathy abolishes presynaptic spike width modulation by subthreshold somatic depolarization. *Proc Natl Acad Sci U S A*. 2017;114(9): 2395–2400.
49. Holth JK, Bomben VC, Reed JG, et al. Tau loss attenuates neuronal network hyperexcitability in mouse and Drosophila genetic models of epilepsy. *J Neurosci*. 2013;33(4):1651–1659.
50. Yuan H, Yuan H, Wang Q, et al. Two novel KCNA1 variants identified in two unrelated Chinese families affected by episodic ataxia type 1 and neurodevelopmental disorders. *Mol Genet Genomic Med*. 2020;8(10):e1434.
51. Verdura E, Fons C, Schlüter A, et al. Complete loss of KCNA1 activity causes neonatal epileptic encephalopathy and dyskinesia. *J Med Genet*. 2020;57(2):132–137.
52. D'Adamo MC, Liantonio A, Rolland J-F, Pessia M, Imbrici P. Kv11 channelopathies: Pathophysiological mechanisms and therapeutic approaches. *Int J Mol Sci*. 2020;21(8):2935.
53. Allen NM, Weckhuysen S, Gorman K, King MD, Lerche H. Genetic potassium channel-associated epilepsies: Clinical review of the Kv family. *Eur J Paediatr Neurol*. 2020;24:105–116.
54. Tottene A, Conti R, Fabbro A, et al. Enhanced excitatory transmission at cortical synapses as the basis for facilitated spreading depression in Ca(v)2.1 knockin migraine mice. *Neuron*. 2009; 61(5):762–773.
55. Yeung SYM, Greenwood IA. Electrophysiological and functional effects of the KCNQ channel blocker XE991 on murine portal vein smooth muscle cells. *Br J Pharmacol*. 2005;146(4):585–595.
56. Gunthorpe MJ, Large CH, Sankar R. The mechanism of action of retigabine (ezogabine), a first-in-class K + channel opener for the treatment of epilepsy. *Epilepsia*. 2012;53(3):412–424.
57. Provence A, Angoli D, Petkov GV. K_V 7 channel pharmacological activation by the novel activator ML213: Role for heteromeric K_V7.4/K_V7.5 channels in guinea pig detrusor smooth muscle function. *J Pharmacol Exp Ther*. 2018;364(1):131–144.
58. Otto JF, Kimball MM, Wilcox KS. Effects of the anticonvulsant retigabine on cultured cortical neurons: Changes in

electroresponsive properties and synaptic transmission. *Mol Pharmacol*. 2002;61(4):921–927.
59. Treven M, Koenig X, Assadpour E, et al. The anticonvulsant retigabine is a subtype selective modulator of GABAA receptors. *Epilepsia*. 2015;56(4):647–657.
60. Main MJ, Cryan JE, Dupere JR, Cox B, Clare JJ, Burbidge SA. Modulation of KCNQ2/3 potassium channels by the novel anticonvulsant retigabine. *Mol Pharmacol*. 2000;58(2):253–262.
61. Jaeger HM, Pehlke JR, Kaltwasser B, et al. The indirect NMDAR inhibitor flupirtine induces sustained post-ischemic recovery, neuroprotection and angioneurogenesis. *Oncotarget*. 2015;6(16): 14033–14044.
62. Bierbower SM, Choveau FS, Lechleiter JD, Shapiro MS. Augmentation of M-type (KCNQ) potassium channels as a novel strategy to reduce stroke-induced brain injury. *J Neurosci*. 2015;35(5):2101–2111.
63. Tzour A, Leibovich H, Barkai O, et al. KV 7/M channels as targets for lipopolysaccharide-induced inflammatory neuronal hyperexcitability. *J Physiol*. 2017;595(3):713–738.
64. Chen S, Yaari Y. Spike Ca2 + influx upmodulates the spike afterdepolarization and bursting via intracellular inhibition of KV7/M channels. *J Physiol*. 2008;586(5):1351–1363.
65. Barrese V, Taglialatela M, Greenwood IA, Davidson C. Protective role of Kv7 channels in oxygen and glucose deprivation-induced damage in rat caudate brain slices. *J Cereb Blood Flow Metab*. 2015; 35(10):1593–1600.
66. Soh H, Park S, Ryan K, Springer K, Maheshwari A, Tzingounis AV. Deletion of KCNQ2/3 potassium channels from PV + interneurons leads to homeostatic potentiation of excitatory transmission. *Elife*. 2018;7:e38617.
67. Losi G, Cammarota M, Carmignoto G. The role of astroglia in the epileptic brain. *Front Pharmacol*. 2012;3:132.
68. Lv S, Guo Z-N, Jin H, et al. Compromised Dynamic Cerebral Autoregulation in Patients with Epilepsy. *BioMed Res Int*. 2018; 2018:6958476.
69. Hascoet JM, Monin P, Vert P. Persistence of impaired autoregulation of cerebral blood flow in the postictal period in piglets. *Epilepsia*. 1988;29(6):743–747.
70. Pescador Ruschel MA, De Jesus O. Migraine headache. *StatPearls*. StatPearls Publishing; 2020. Updated 7 July 2021. http://www.ncbi.nlm.nih.gov/books/NBK560787/
71. Leao AAP. Spreading depression of activity in the cerebral cortex. *J Neurophysiol*. 1944;7(6):359–390.
72. Golomb D, Yue C, Yaari Y. Contribution of persistent Na + current and M-type K + current to somatic bursting in CA1 pyramidal cells: Combined experimental and modeling study. *J Neurophysiol*. 2006;96(4):1912–1926.
73. Glasscock E, Qian J, Kole MJ, Noebels JL. Transcompartmental reversal of single fibre hyperexcitability in juxtaparanodal Kv1.1-deficient vagus nerve axons by activation of nodal KCNQ channels. *J Physiol*. 2012;590(16):3913–3926.
74. Sampath D, Lam PM, Laoprasert M, et al. Effects of a potassium channel opener on brain injury and neurologic outcomes in an animal model of neonatal hypoxic-ischemic injury. *Pediatr Res*. 2020;88(2):202–208.
75. Vigil FA, Bozdemir E, Bugay V, et al. Prevention of brain damage after traumatic brain injury by pharmacological enhancement of KCNQ (Kv7, "M-type") K + currents in neurons. *J Cereb Blood Flow Metab*. 2020;40(6):1256–1273.
76. Brown DA, Adams PR. Muscarinic suppression of a novel voltage-sensitive K + current in a vertebrate neurone. *Nature*. 1980; 283(5748):673–676.
77. Abbott GW. KCNQs: Ligand- and voltage-gated potassium channels. *Front Physiol*. 2020;11:583.
78. Klass A, Sánchez-Porras R, Santos E. Systematic review of the pharmacological agents that have been tested against spreading depolarizations. *J Cereb Blood Flow Metab*. 2018;38(7): 1149–1179.
79. Aiba I, Shuttleworth CW. Characterization of inhibitory GABA-A receptor activation during spreading depolarization in brain slice. *PLoS One*. 2014;9(10):e110849.
80. Desroches M, Faugeras O, Krupa M, Mantegazza M. Modeling cortical spreading depression induced by the hyperactivity of interneurons. *J Comput Neurosci*. 2019; 47(2-3):125–140.